Article

Land-Atmosphere Transfer Parameters in the Brazilian Pantanal during the Dry Season

Paolo Martano [1],*, Edson Pereira Marques Filho [2] and Leonardo Deane de Abreu Sá [3]

[1] CNR Istituto di Scienze dell'Atmosfera e del Clima, UOS Lecce, Via Monteroni, Lecce 73100, Italy

[2] Universidade Federal da Bahia, Instituto de Física, Departamento de Física da Terra e do Meio Ambiente, Travessa Barão de Jeremoabo, s/n, Campus Ondina, Salvador 40170-280, BA, Brazil; E-Mail: edson.marques@ufba.br

[3] Centro Regional da Amazônia, Instituto Nacional de Pesquisas Espaciais (INPE), Parque de C. & T. do Guamá, Av. Perimetral 2651, Lote 50, Belém 66.077-830, Pará, Brazil; E-Mail: leonardo.deane@inpe.br

* Author to whom correspondence should be addressed; E-Mail: p.martano@isac.cnr.it; Tel.: +39-083-229-8718; Fax: +39-083-229-8716.

Academic Editors: Daniele Contini and Robert W. Talbot

Abstract: The Brazilian region of Pantanal is one of the largest wetlands in the world, characterized by a wet season, in which it is covered by a shallow water layer, and a dry season, in which the water layer disappears. The aim of this study is the estimation of the main parameters (drag coefficients and surface scale lengths) involved in modelling the surface atmosphere transfer of momentum, heat and water vapor from the dataset of the second Interdisciplinary Pantanal Experiment (IPE2). The roughness parameters and the stability correction parameters have been estimated in the framework of the similarity theory for the vertical profiles of wind speed and temperature. Thus, a previously-developed methodology was adapted to the available dataset from the IPE2 five-level mast. The results are in reasonable agreement with the available literature. An attempt to obtain the scalar transfer parameters for water vapor has been performed by a Penman–Monteith approach using a two-component surface resistance in parallel between a vegetation and a bare soil part. The parameters of the model have been calibrated using a non-linear regression method. The scalar drag coefficient retrieved in this way is in agreement with that calculated by the flux-gradient approach for the sensible heat flux. Eventually, an evaluation of the vegetation contribution to the total vapor flux is given.

1. Introduction

The Earth's surface is a continuous sink of momentum flux by friction and a source/sink of heat and water vapor (scalar) fluxes from the atmospheric flow over it. The connection between these turbulence-driven fluxes and the mean vertical profiles of the atmospheric variables (wind speed, temperature and humidity) is established by a few parameters that characterize the local surface response and the effect of the local atmospheric stratification. In the framework of Monin–Obukhov (MO) similarity [1], the surface responses for momentum and scalar fluxes are described by bulk drag coefficients that depend on the measurement height z and on the atmospheric stability described by the MO length L. The measurement height is scaled by the roughness length z_0 and subjected to a displacement height d, and the atmospheric stability is a function of z/L that depends on at least one additional parameter (stability function parameter a). The surface length parameters z_0 and d are naturally site-dependent, and also the stability parameter a, in principle not depending on the surface characteristics, has shown some variability for measurements taken at different experimental sites [1].

The determination of these parameters is of basic importance for many applications. In meteorological modelling, they represent the necessary boundary conditions for large-scale and mesoscale models [2], and the roughness length scales directly influence the development of global atmospheric circulations and the development of synoptic storms [3,4]. In atmospheric pollution modelling, they describe the surface turbulence conditions [5], thus directly affecting the vertical diffusion of the pollutant plumes [6]. Efforts to generate global mappings of the roughness length by satellite-derived data have been made in past years [7], but local validation by experimental measurements are not always available everywhere.

In the past few years, different techniques have been used to calculate the mentioned parameters in several dedicated experiments at different sites. Generally, the roughness parameters for wind speed are calculated by vertical wind speed profiles selected as close as possible to neutral atmospheric stability [8]. In practical applications, the temperature (scalar) roughness lengths have been often considered as equal to the momentum roughness, thus needing the introduction of an "aerodynamic surface temperature" as the surface boundary condition, which is different from the measured radiative surface temperature (brightness temperature). The aerodynamic temperature is, however, not operationally well defined in order to be experimentally determined [9]. If the measured radiative surface temperature is used instead (by airborne or satellite measurements), then the roughness scalar length z_{0T} is different from z_0, and the correction term in the temperature profile $kB = ln(z_0/z_{0T})$ is generally parameterized with different expressions for different surface roughness conditions, mainly validated in wind tunnel experiments [1]. The case is more complicated for the surface vapor flux, as the humidity profile has a surface value that is often not experimentally measurable at all.

The displacement height is usually experimentally determined from neutral wind profiles together with the roughness length, but alternative methods to determine it have also been proposed [10].

However, these methods make use of other experimentally-obtained parameters that must be known, including their uncertainty in the results. In addition, the displacement height is considered to be the same for scalars and momentum, as usual in practical uses, although it has been pointed out that no theoretical reasons exist for this assumption, because momentum and heat transfer have physically different mechanisms [11]. Martano [12] (referred to as M00) proposed a simple direct mathematical procedure to obtain both the roughness and the displacement height for momentum from single-level sonic anemometer data in all stability conditions, together with an estimation of their experimental uncertainties.

The stability parameters are usually experimentally determined in a separate and different way, because they are directly linked to the vertical gradients in the wind/scalar profiles. In their classical approach, Businger *et al.* [13] locally fit the vertical profiles measurements by a polynomial regression and retrieved the local vertical gradients by differentiation of the local regression curve at each measurement level. The stability parameter is then obtained by fitting the stability function over the obtained gradient profile values at all measurement levels.

In the following approach, the roughness parameters together with the stability parameter are determined simultaneously by a minimum least squares approach over a couple of levels for wind speed and temperature profiles separately. This is obtained by a modification of the M00 approach, extending it to a couple of levels, averaging the obtained results over all available levels and applying it to both the wind speed and the temperature profiles (with the radiative temperature as the surface boundary condition). This allows, in principle, a best-fit of the roughness and stability parameters simultaneously, for either the wind profile or the temperature profiles, in all stability conditions, and an estimate of the parameters' uncertainty from the scatter for different couples of levels. The undefined surface boundary condition prevents the application of this method to the water vapor profile. In this case, for the sake of completeness, the surface drag coefficient for the water vapor has been calculated applying a Penman–Monteith (PM) approach [1], with a procedure that needs a minimum requirement of surface information [14].

This study is applied to a dataset from an experimental campaign in the Pantanal wetland, a very large plane area in the central Brazil that is of great importance for the correct meteorological modelling over the South American continent, but with a limited amount of *in situ* meteorological experimental facilities. The aim is to apply the flux-profile relations for the wind speed and the temperature and the Penman–Monteith equation for the evapotranspiration flux to obtain estimates of the surface roughness parameters and the drag coefficients. These parameters are of main importance in modelling the local boundary layer in this region, also for practical purposes as meteorological modelling and air quality modelling for fire plumes and pollution dispersion [2,5].

2. Site, Experiment and Dataset

The Brazilian Pantanal is considered the largest watered plane area in the world, located in the middle of Brazil, west of Mato Grosso do Sul and, also, including part of Paraguay and Bolivia. It consist of an area of more than 130,000 km^2, periodically flooded by the Rio Paraguay and its affluents. Its surface shows an extremely large variability of conditions during the annual cycle, passing from very dry conditions (dry season: April–October), with actual fire risk ("*queimadas*"), to

almost lagoon conditions (wet season: November–March), covered by a water layer that can reach several tens of centimeters in height. The climate is classified between sub-humid and semiarid with annual precipitations between 1000 and 1400 mm, mostly concentrated in the wet season. Temperature can reach 40 °C in summer, but can decrease down to 0 °C in winter, in association with cold fronts passing over the region. Due to the extension and the large seasonal variability, the vegetation cover is heterogeneous, including a large quantities of gramineous plants and bushes and different types of trees up to 20 meters in height.

Due to these typical characteristics, the climatic importance and the extension of the region, in 1986, a large research program for the Pantanal region was implemented [15]. Within this program, a series of four experimental campaigns were implemented for better knowledge of the interaction between climatic microclimatic hydrologic and ecologic characteristics of the region between 1998 and 2002 (Interdisciplinary Pantanal Experiments: IPE0, IPE1, IPE2, IPE3). The National Institute for Space Research (Instituto Nacional de Pesquisas Espaciais (INPE)) and the Federal University of Mato Grosso do Sul (Universidade Federal do Mato Grosso do Sul (UFMS)) collaborated in the climatic and microclimatic studies and experiments, including the implementation of a micrometeorological tower of 22 meters in height for data collection in the dry and in the wet season. The aim was also to collect information about the surface-atmosphere turbulent exchanges during different seasons in view of their importance for the regional climate and the local ecosystem characteristics and variability [15].

This work concerns the analysis of data collected in the IPE2 campaign of about two weeks in the dry season. The dataset was collected in September 1999 by a micrometeorological tower located at 19°33′53″S, 57°01′06″W, in the Fazenda São Bento, next to the Pantanal project base of UFMS, in a clear plane not far from the embankments of the Miranda River (Figure 1). At less than 1 km south of the tower, the embankment canopy of the Miranda River dominates the landscape, while in the north and west direction, medium–tall bushes and trees dominate (mainly "*paratudo*", typical Pantanal trees of maximum 10 m in height, flowering just in this period of the year). In the east direction, the soil is mainly covered by gramineous plants. North and south views from the measurement site are shown in Figure 2. The tower was 24 m in height with five levels of measurements at 8, 10, 14, 16 and 22 m in height. All levels were equipped with a standard anemometer (VECTOR A100LK) and a psychrometer (implemented by two CAMPBELL TEMP 107 thermistors) for wind speed, temperature and humidity measurements. In addition, the highest level was equipped with a sonic anemometer (CAMPBELL CSA-T3), and a net radiometer with separate long- and short-wave components (KIPP & ZONEN CNR1) was located at 4 meters height in the same tower. Two soil heat flux plates (REBS HFT3) were located at the base of the tower at a 2- and 5-cm depth, and six soil thermometers (CAMPBELL TEMP107) were located at a 1-, 2-, 5-, 10-, 20- and 40-cm depth. However, not all sensors were properly working during all of the measurement periods. More details about the experimental site and equipment and the campaigns can be found elsewhere [16–19]. After an accurate data check that discarded a consistent amount of wrong and dubious measurements mainly associated with sensors malfunctioning, about one week of measurements was retained, in the period between 17 and 22 September, which have been used for the present analysis. No gap filling in the measured time series has been used, this not being necessary for the following methodology.

Figure 1. Map of the experimental site.

Figure 2. North (**left**) and south (**right**) view from the micrometeorological tower.

3. Methodology

3.1. Wind Speed and Temperature

The roughness parameters for heat and momentum have been estimated starting from the M00 approach [12]. It looks for the minimum of the variance of $S(z_0,d) = kU/u^* + \Psi((z - d)/L) - \Psi(z_0/L)$ over the measurement dataset, which is a two-parameter minimization problem for z_0 and d, and reduced it to a one-parameter conditioned minimization problem that is straightforward to solve

numerically. (here, $u*$ is the friction velocity, U the wind speed, k the Von Karman constant and Ψ the stability function of the measurement height z and the MO length L [1]). The M00 approach was originally developed for single-level sonic anemometer measurements; thus, some changes have been made to adapt it to the different condition of a multi-level slow response sensor mast. Indeed, the information available for five levels of slow response measurements has been used to look for an estimation of the stability parameter together with the roughness parameters. Then, the M00 approach has been modified to be used with couples of measurement levels together with the turbulent fluxes estimated by the fast response measurements on the mast top, in the following way.

As in M00, the parameters are again estimated through the minimization of the statistical variance $\sigma_S{}^2 = \langle (S - \langle S \rangle)^2 \rangle$, where S is now defined as a function of d and the stability parameter a:

$$S(d,a) = k\Delta q/q* + \Psi((z_2 - d)/L,a) - \Psi((z_1 - d)/L,a) \tag{1}$$

that is again a two-parameter minimization problem.

Here, Δq represents the difference of the measured quantities (either the wind speed U or the virtual potential temperature Θ_v in the present case) between the two considered measurements levels z_1 and z_2, $q*$ is the turbulent scale of q obtained from the fast response measurements, $\Psi((z_1 - d)/L,(z_2 - d)/L)$ is the stability function depending on the displacement height d and an unknown stability parameter a, also to be determined (see the end of this section), k is the Von Karman constant ($k = 0.4$) and $\langle \ldots \rangle$ represents the average over the dataset [12].

In a way totally analogous to that of M00, it can be shown that the expected value of a can be found minimizing $\sigma_S{}^2$ with respect to a only, with d calculated by the following constraint:

$$d = (z_1 exp\langle S(d,a) \rangle - z_2)/(exp\langle S(d,a) \rangle - 1) \tag{2}$$

from which d is also found numerically solving the above equation. Thus, it is straightforward to find the minimum of $\sigma_S{}^2$ with respect to a, just numerically evaluating $\sigma_S{}^2$ with a changing step by step between fixed maximum and minimum values and recalculating d by Equation (2) at each step. The estimates of a and d are obtained when the minimum of $\sigma_S{}^2$ is found. Some examples of the procedure are shown in Figure 3.

Now, it is possible to obtain the estimated z_0 (for the variable q) using a and d to numerically solve the equation:

$$ln((z - d)/z_0) = \langle k\Delta q_0/q* + \Psi((z - d)/L,a) - \Psi(z_0/L,a) \rangle \tag{3}$$

where Δq_0 is the difference between $q(z)$ and the surface value q_0 of q (that is, U or Θ_v). Alternatively, the M00 approach can be used to determine both d and z_0 using the estimated value of a. Both methods have been used in the following sections for comparison.

The classical Businger–Dyer stability functions [1] for the wind speed U and the potential temperature Θ have been used here (stable condition: $L > 0$, unstable condition: $L < 0$):

$$\Psi_U(x,a) = 2ln[(1 + y)/2] + ln[(1 + y^2)/2] - 2tan^{-1}x + \pi/2 \tag{4}$$

where $y = (1 - ax)^{1/4}$ in the unstable condition;

$$\Psi_\Theta(x,a) = 2ln[(1 + y)/2] \tag{5}$$

where $y = (1 - ax)^{1/2}$ in the unstable condition;

$$\Psi_{U,\Theta}(x,a) = -ax \tag{6}$$

in the stable condition.

More details about the similarity flux-profiles relations and the parameter values *a* for different meteorological variables and stability conditions can be found in [1].
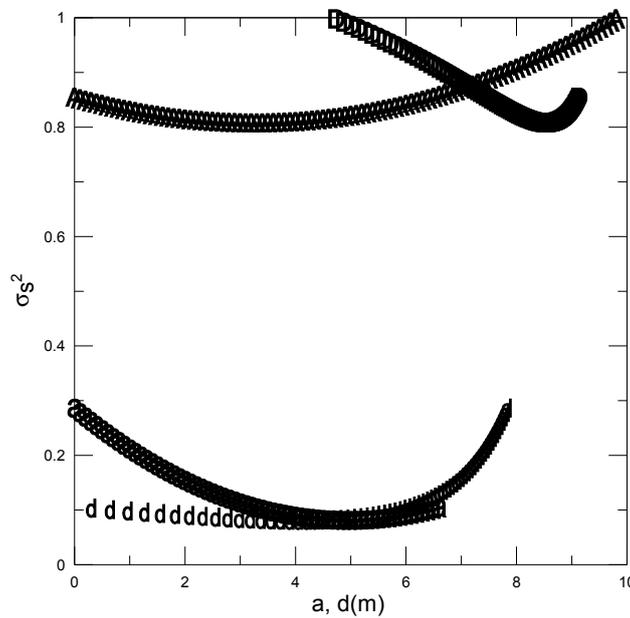

Figure 3. Example of σ_S^2 (Equation (1)) for ΔU and for $\Delta\Theta_v$ calculated as a function of *a* (symbols: **a** for ΔU and **A** for $\Delta\Theta_v$) and of *d* (symbols: **d** for ΔU and **D** for $\Delta\Theta_v$), for the couple of Levels 2–3. The abscissa of the minima represents the estimated value of *a* and *d* for ΔU and for $\Delta\Theta_v$ in each case.

3.2. Water Vapor

The Penman–Monteith (PM) approach has been used to obtain an estimate of the scalar drag coefficient for the water vapor, as the surface value q_0 is not available for the water vapor. A "hybrid" formulation of the PM model was proposed by Martano [14] in which a surface resistance can be expressed by the parallel between a soil surface resistance R_s and a canopy resistance R_v. This is supposed to be the simplest way to capture the main characteristics of partially-vegetated surfaces, with bare soil and vegetated surfaces giving independent contributions to the total evaporation, and is justified by the lack of detailed surface information. Indeed, this model has the advantage of almost no necessity of additional surface information besides the regression parameters themselves, and actually, no additional external parameter is needed in the following procedure (e.g., no LAI value is used). For the sake of completeness, a short description follows.

The modelled latent heat flux Q_{em} is expressed in the PM model as [1]:

$$Q_{em} = [sE + \rho C_p q_{sat} (1 - H_r)/R_a][s + \gamma(1 + R_0/R_a)]^{-1} \tag{7}$$

where H_r is the air relative humidity, q_{sat} the saturation-specific humidity, E the measured available energy flux (net radiation minus soil heat flux), s the slope of the saturation curve (from the Clapeyron formula), γ the psychrometric constant and C_p and ρ the specific heat and the density of the air. All

variables in the right-hand side are measured, with the exception of the surface resistance R_0 and the aerodynamic resistance R_a. R_a is expressed by a scalar drag coefficient C_h that is considered as an unknown parameter to be determined in the form [1]:

$$R_a = (C_h\,U)^{-1} \tag{8}$$

In partially-vegetated areas, the generalized surface resistance R_0 can be expressed as a parallel independent resistance contribution of the vegetated and the non-vegetated surface fractions, respectively R_v and R_s:

$$1/R_0 = 1/R_s + 1/R_v \tag{9}$$

The soil resistance R_s, is a strongly nonlinear function of the soil-specific water content w. It is modelled following the expression given by Kondo and Saigusa [20] for a "wetness parameter" that is mathematically equivalent to a surface resistance parameter. Using this equivalence, the surface resistance can be expressed as [14,20]:

$$R_s = C_s/D_a\,(w_{sat} - w)^p \tag{10}$$

where w_{sat} is the saturation-specific water content, $D_a = 0.000023(T_s/273.2)^{1.75}$, T_s is the soil surface temperature, C_s is an unknown parameter depending on the soil texture and the actual non-vegetated fraction of the surface and $p = 10$ for loamy soil [20].

Rana *et al.* [21] developed a simple model, in which the resistance of the vegetated surface R_v depends on the available energy and the air humidity through a similarity resistance form R_*:

$$R_* = \rho L e q_{sat}(1 - H_r)(1 + \gamma/s)/E \tag{11}$$

that is $R_v/R_a = f(R_*/R_a)$, and used a linear approximation for the function f. Accordingly, the following expression is proposed for the vegetated fraction [14]:

$$R_v/R_a = C_v\,R_*/R_a \tag{12}$$

where C_v is a parameter depending on the vegetation characteristics and the effective contribution of the vegetated surface fraction to the evapotranspiration.

From Equation (7) and using Equations (8)–(12), the latent heat flux can be expressed by measurements of air temperature and humidity, soil moisture, wind speed and available energy flux (net radiation minus soil heat flux), plus three unknown parameters, C_h, C_v and C_s. These determine the effective scalar drag coefficient and the evaporative response of the vegetated and non-vegetated fractions of the surface, respectively.

4. Parameter Estimation and Discussion

4.1. Temperature and Wind Speed: Estimation of the Surface Length Scales and the Stability Parameter

Equation (1) was used to calculate $\sigma_S^2 = \langle(S - \langle S\rangle)^2\rangle$ incrementing step by step the value of the parameter a, with d calculated by numerically solving Equation (2).

Figure 3 shows an example of the curves obtained for σ_S^2 as a function of d and a, both for the wind speed and the temperature for the couple of Levels 2 and 3.

The results for the values of a, d and z_0 are shown in Table 1 for the couples of levels where a minimum of σ_S^2 has been found. The surface value of the temperature T_{0e} ($T_{0e} = q_0$ in Equation (3)), has been estimated by the measured long wave upward emission Rl_e considered as blackbody emission ($Rl_e = \sigma T_{0e}^4$), as no estimate was available for the soil surface emissivity. The radiometer was located at a four-meter height, which implies a field of view radius of about 40 meters (which captures about 99% of the total contribution to the surface flux [22]). Although much larger than the field of view of a typical infrared thermometer, this can be still significantly less than the flux footprint at the top tower level (see Section 4.3).

An estimation of the uncertainty introduced by the blackbody approximation is given in the Appendix and is expected not to be greater than that associated with the difference between the radiometer field of view and the footprint area of the turbulent fluxes [14]. The uncertainty in the average values of Table 1 has been estimated as the standard deviation of the values obtained for all different couples of levels; although the estimated uncertainty by the M00 method for each value associated with a couple of a level is quite larger and of the order of the parameter value. This can be somehow expected from the results in the Appendix, where an estimation of the experimental uncertainty of the temperature roughness length z_{0T} is given. The average values of a are in reasonable agreement with the literature ($a \approx 16$ unstable; $a \approx 4.7$ stable [1]), taking into account the statistical errors, in the case of the wind speed. For the potential temperature, a is underestimated, but the uncertainty in the measurements is greater in this case; and there is no result obtained for Θ_v in the unstable case, in which the measured vertical temperature differences can be hardly significant due to the strong turbulent mixing.

Table 1. a, d and z_0 calculated from the shown couples of levels for U and Θ_v (Equations (1)–(3)).

Levels	a	d (m)	z_0 (m)
U Stable			
1–3	4.5	1.9	0.13
1–5	4.1	3.7	0.07
2–3	4.9	4.2	0.09
2–5	4.2	5.3	0.06
3–5	3.8	6.9	0.04
Averages	4.3 ± 0.4	4.4 ± 1.8	0.08 ± 0.03
U Unstable			
1–3	10.2	2.7	0.05
Θ_v Stable			
1–2	3.0	3.6	0.17
1–3	1.4	6.9	0.03
2–3	3.3	8.5	0.03
Averages	2.6 ± 1.0	6.3 ± 2.5	0.08 ± 0.08

The results of the evaluation of z_0 and d by the M00 method are reported for comparison in Table 2 for each measurement level, using the average values of a from Table 1.

The results for the wind speed are in reasonable agreement between Table 1 and Table 2, in the stable case, while in the unstable case, they do not compare well (for the wind speed). Again, this could be related to the larger uncertainty connected to the enhanced turbulent fluctuations in the data, but also to the strong reduction of the footprint in the unstable case. This can enhance the effect of the terrain heterogeneities over the change of footprint due to the different heights of the measurement levels (Section 4.3). However, some independent estimations by a different method applicable in free convection [10] give average values for *d* of about 5 m, in agreement with the results reported here for the stable case.

Table 2. *d* and z_0 calculated as in M00 (Martano approach), with average values of *a* from Table 1.

|	*U Stable*				
Levels	1	2	3	5	Averages
z_0 (m)	0.07	0.08	0.09	0.07	0.08 ± 0.01
d (m)	3.8	4.1	3.5	4.4	4.0 ± 0.4
	U Unstable				
Levels	1	2	3	5	Averages
z_0 (m)	0.017	0.024	0.017	-	0.019 ± 0.004
d (m)	6.8	7.7	11.0	-	8.5 ± 2.2
	Θ_v *Stable*				
Levels	1	2	3	5	Averages
z_0 (m)	0.12	0.13	0.08	-	0.11 ± 0.03
d (m)	4.8	4.8	4.9	-	4.8 ± 0.1
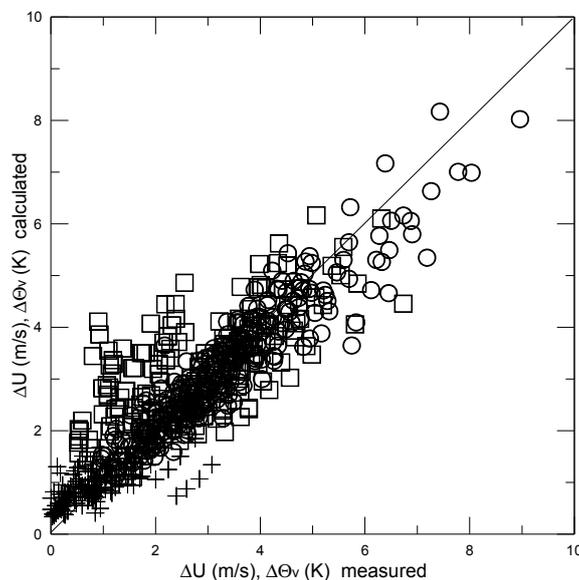
Figure 4. Test for ΔU (stable: circles, unstable: squares) and $\Delta \Theta_v$ (+) calculated between the surface and all measurement levels by the similarity profiles with the averaged parameters in Table 1, *versus* the measured values.

In principle, although often assumed in practical applications, there is no "*a priori*" reason for which *d* and z_0 should be equal for different physical quantities, the surface transfer for wind speed,

temperature and scalars being governed by different physical processes. In general, z_0 could depend also on the flow condition [1], and a theoretical analysis gives different expressions for d in the case of wind speed and temperature [11]. Nevertheless, within the relevant uncertainty in the temperature parameters (Table 1 and the Appendix), the obtained results do not point out relevant differences in z_0 and d between wind speed and temperature, at least in order of magnitude and for stable conditions.

There is a general trend with the height of the measurements levels in the estimated values of d, possibly related to the heterogeneities in the ground surface characteristics (bushes and trees areas) at increasing fields of view. Nevertheless, the values of d obtained from different heights have been averaged (as for a and z_0) to test the ability of the average values of a, d and z_0 in reproducing the observed profiles for the wind speed and the potential temperature. The results are shown in Figure 4, where the values of U and $\Delta\Theta_v$ have been calculated using the averaged values of a, d and z_0 from Table 1 and compared with the measured data for all measurement levels. The agreement is fairly good, mainly for the wind speed in the stable case, while a larger dispersion is present for the temperature and the wind speed in the unstable case, as expected.

4.2. Water Vapor: Estimation of the Scalar Drag Coefficient

The previous approach is not applicable to the humidity profile and the latent heat flux, due both to the difficulties in determining a "surface value" q_0 for the air humidity [1] and the large uncertainty in the humidity gradients estimated between the measurement levels. Instead, to obtain an estimate of the surface transfer coefficients, the approach outlined in Section 3.2 has been used together with the regression method described in [14], which will be shortly outlined here. To estimate the unknown parameters C_h, C_v and C_s for the simple model outlined in Section 3.2, a cost function F depending on both the latent heat flux and the surface temperature is written in the form [14]:

$$F(C_h, C_v, C_s) = (2N)^{-1} \sum_1^N ([Q_e - Q_{em}(C_h, C_v, C_s)]^2/\sigma_Q^2 + [\Delta\Theta_{v0} - \Delta\Theta_{vm}(C_h, C_v, C_s)]^2/\sigma_\Theta^2) \quad (13)$$

where Q_e represents the experimental latent heat flux data, estimated as $Q_e = E - Q_s$ (the difference between the measured net radiation, soil heat flux and measured sensible heat flux Q_s), thus assuming the surface energy budget closure. $\Delta\Theta_{v0}$ is the measured surface-atmosphere potential virtual temperature difference (depending on the considered level of measurement) from a dataset of N measurements. The modelled temperature difference $\Delta\Theta_{vm}(C_h, C_v, C_s)$ is expressed using the energy budget closure, the modelled latent flux Q_{em} (Equation (1)) and the drag laws [1,14] as:

$$\Delta\Theta_{vm}(C_h, C_v, C_s) = [E - Q_{em}(C_h, C_v, C_s)]/(C_p \rho U C_h) \quad (14)$$

The expected statistical uncertainties σ_Q, σ_T for Q_e and Θ_v have been chosen as 30 W·m^{-2} and 3 K, respectively. The first value comes from an evaluation of the instrumental errors and is in general agreement with an expected uncertainty coming from the flux estimation by the energy budget [23]. The second comes from a calculation of the variance between the radiometric surface temperature estimate and the soil temperature at a 1-cm depth. It is also comparable with other estimates obtained elsewhere [14,24], and this choice for the statistical uncertainties is in agreement with the obtained convergence values for F that are expected to be close to one [24].

Being based on the PM equation, the model assumes the closure of the surface energy budget and the identity between the scalar transfer coefficient C_h for heat and water vapor.

The Bowen ratio for the measurement period, which appears to be often close or even less then unity [25], indicates a permanent, strong evaporative contribution to the surface heat transfer also in the dry season. Then, lacking an experimental estimation for the soil moisture content and taking into account that the chosen dataset is of a few days at the end of the dry season without relevant precipitation, a constant value for the surface soil moisture has been adopted here. However, the chosen value of the constant soil moisture, as well as the other soil constants should not affect the final results, because the parameter C_s in Equation (10) is adjusted by the regression procedure (the values used were $w = 0.3$ and $w_s = 0.49$ with $p = 10$ [20]). Eventually, the function F has been minimized by the Levenberg–Marquardt regression method [24,26] for the measurement Levels 3 and 5.

In Table 3, Column 1, the results obtained for the scalar drag coefficient C_h for the same Levels 3 and 5 are reported. In Column 2, they have been calculated from the experimental data of temperature and heat flux (flux-gradient approach), as averaged values of the scalar drag for the sensible heat transfer in the unstable case. They can also be compared with the values obtained from the averages of z_0 and d from Table 1 and calculated as $C_h = k^2[(ln(z - d)/z_0)(ln(z - d)/z_{0T})]^{-1}$ [1], which are 7.5×10^{-3} and 5.6×10^{-3} for Levels 3 and 5, respectively (stable case). Figures 5 and 6 test the reliability of the obtained parameters by plotting the parameterized *versus* the measured latent heat fluxes and surface-air temperature differences from Levels 3 and 5 during the daytime. Both have a fairly good correlation, but with a larger scatter in the case of the temperature differences. This is somehow expected, as the PM model itself is derived by an approximation that eliminates the surface temperature from the expression of the latent flux [1], thus not being directly sensitive to this parameter.

Table 3. C_h from both the Penman–Monteith (PM) model and measurements and the evaporative vegetation fractions (*evf*).

Level	C_h PM Model (10^{-3})	C_h Data Average (10^{-3})	*evf*
3	7.6 ± 1.5	6.8 ± 0.4	0.72 ± 0.11
5	6.5 ± 1.2	5.4 ± 0.3	0.83 ± 0.08

Finally, Column 3 of Table 3 shows an estimate of the averaged fractional contribution to the latent heat flux for the vegetation fraction (*evf*) in the parallel resistances model approximation. Defining the latent flux contribution from either bare soil or the vegetation fractional areas as Q_{es} and Q_{ev}, respectively, it is straightforward to show that $Q_{es}/Q_e = (R_s//R_v)/R_s$ and $Q_{ev}/Q_e = (R_s//R_v)/R_v$ (with the obvious condition $Q_{es}/Q_e + Q_{ev}/Q_e = 1$). The results show that the vegetated areas should be responsible for 70%–80% of the latent heat flux in the dry season. Thus, the vegetation has a dominant contribution, even in the presence of the quite large soil moisture content that is expected from the generally small values of the Bowen ratio in the whole period of measurements.

4.3. Discussion

Eventually, two more aspects should be addressed, which are related to the reliability of the obtained parameters. The first aspect consist of the validity of the similarity profiles at the considered measurement heights. It is well known that MO similarity profiles are based on some equilibrium assumptions about the turbulence in the boundary layer that actually exist above a "roughness sublayer" of height z_r over the roughness elements. A discussion can be found in [8], where a

suggested expression for z_r is proposed as $z_r = d + 20z_0$, allowing a test of the self-consistency of the obtained length scales. Thus, using the results for z_0 and d, it is found $z_r \approx 7$ m, still below the tower lower measurement level of 8 m, which means that the obtained results are consistent with the measurement level heights.
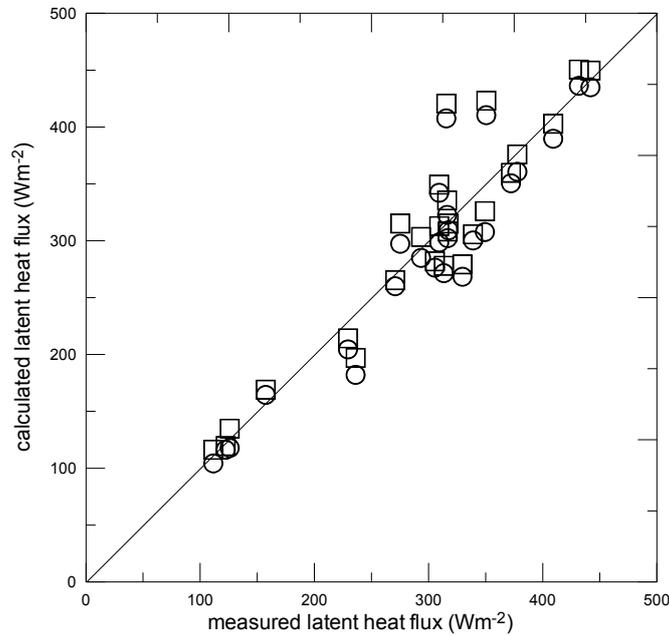

Figure 5. Test for the latent heat flux calculated by the PM model with the calibrated parameters, *versus* the latent heat flux estimated by the measured surface energy budget (squares: Level 3, circles: Level 5).
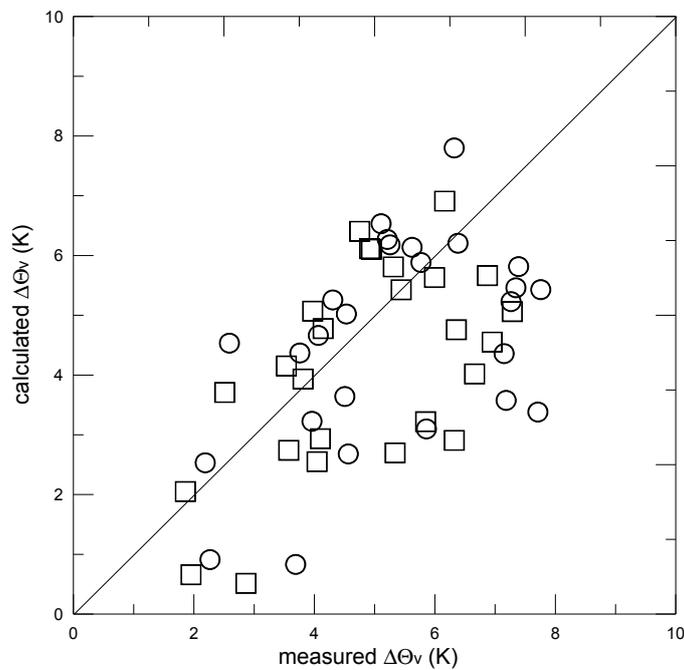
Figure 6. Test for $\Delta\Theta_v$ obtained by the PM model with the calibrated parameters *versus* the measured values (squares: Level 3, circles: Level 5).

The second aspect concerns the spatial representativeness of the estimated values, which is related to the spatial source area for the measured turbulent fluxes. An estimation of the flux footprint for the different tower levels can be calculated by a simple analytical model as function of d, z_0 and L [27]. Using the estimated values for the surface length scales and typical average values of L for daytime and nighttime from the dataset (nighttime $L \approx 10$ m and daytime $L \approx -10$ m), it results that the 90% flux footprint varies from more than 10 km upwind (nighttime) to about 500 m (daytime) for the upper measurement level and from 2.5 km to about 200 m for the lower level. The strong reduction of the footprint in the daytime may be related to the difficulties in obtaining the transfer parameters for the unstable case, because the heterogeneities of the terrain roughness can be more relevant on this smaller source area and, also, they can show stronger variability with the measurement level. It also appears that the obtained transfer parameters, estimated in the stable case, are representative of an area of some square kilometers around the tower.

5. Summary and Conclusions

Micrometeorological data from measurements of the IPE2 experiment in the Brazilian Pantanal have been analyzed in order to obtain surface-atmosphere transfer parameters. A modification of the M00 [12] method allowed the estimation of the surface roughness length, the displacement height and of a stability function parameter from the measured profiles of wind speed and temperature. This gives consistent results in the stable case, but uncertain results in the unstable case. In particular, no relevant differences have been found in the results for the momentum and the potential temperature transfer parameters in the stable case, although the uncertainty remains quite relevant in the parameter values, especially for the temperature profiles.

The latent heat flux is always a relevant component of the surface energy budget, as the Bowen ratio appears to be often less than unity in the dataset [25]. The scalar transfer coefficients (for water vapor) have been calculated by a Penman–Monteith model, based on three calibration parameters representing the scalar drag coefficient and the evaporative response of the bare soil and the vegetated areas. The obtained scalar drag coefficient is consistent with the average flux gradient value deduced from the temperature and heat flux measurements (in the unstable case) and also consistent with the obtained parameters from the profile analysis in the stable case. Eventually, the model allows an approximate evaluation of the bare soil and the vegetation contribution to the latent heat flux: the vegetation appears to contribute about 70%–80% of the total vapor flux in the dry season.

Acknowledgments

Author Contributions

Martano: methodology, calculations and results. Pereira Marques Filho: data check and data analysis. Abreu Sá: conceived of and designed the experimental campaign and dataset organization.

Conflicts of Interest

The authors declare no conflict of interest.

Appendix

An estimation of the uncertainty for the radiometric surface temperature and, consequently, for the scalar roughness is given in the following.

The total longwave radiation Rl_e measured by a radiometer above a radiant surface of emissivity ε and (real) surface temperature T_0 is due to the surface thermal emission $Rl_0 = \varepsilon\sigma T_0^4$ plus the reflected environment radiation Rl_a and is given by (σ is the Stefan–Boltzmann constant):

$$Rl_e = \varepsilon\sigma T_0^4 + (1 - \varepsilon)Rl_a \tag{A1}$$

Putting $Rl_e = \sigma T_{0e}^4$ and $\alpha = (1 - \varepsilon)/\varepsilon$ where T_{0e} is the estimated "blackbody" surface temperature, it is straightforward to show that, for $\alpha[1 - R]<<1$ and $R = Rl_a/Rl_e$:

$$T_0 = T_{0e}(1 + \alpha - \alpha R)^{1/4} \approx T_{0e}(1 + \alpha[1 - R]/4) \tag{A2}$$

For natural ground surfaces, typically $\varepsilon \geq 0.96$, so that $\alpha \leq 0.04$, and in the whole dataset, it results that $0.8 < R < 1$; then:

$$|T_0 - T_{0e}|/T_{0e} \leq 0.002 \tag{A3}$$

This uncertainty (typically 0.6 K for $T_0 = 300$ K) is comparable with the typical uncertainties of brightness surface temperature from satellite data and comparable or less than the inherent uncertainties associated with the heterogeneities of the surface in the source area containing the footprint of the turbulent fluxes, which can be of some degrees [14].

This uncertainty affects the surface-air temperature difference ΔT by a factor $1 + \beta_T$, which is directly related to the uncertainty factor β on the estimation of the scalar roughness parameter z_{0T}. An approximate flux gradient relation for these uncertainties can be written as:

$$\Delta T(1 \pm \beta_T) \approx (T^*/k)\ln(z/\beta z_{0T}) \tag{A4}$$

Taking into account that $\Delta T \approx (T^*/k)\ln(z/z_{0T})$, it results:

$$\pm k\Delta T\beta_T/T^* \approx \ln(1/\beta) \tag{A5}$$

Inserting the average values from the dataset $\Delta T/T^* \approx 20$ and $\beta_T \approx 0.15$ (calculated as the ratio of the previous estimate of the uncertainty of T_0 of 0.6 K and the average value $|\Delta T| \approx 4$ K), it appears that β can affect the uncertainty of z_{0T} by a factor three.

References

1. Garratt, J.R. *The Atmospheric Boundary Layer*; Cambridge University Press: New York, NY, USA, 1992.
2. Pielke, R.A. *Mesoscale Meteorological Modelling*; Academic Press: London, UK, 2002.
3. Anthes, R.A. Boundary layers in numerical weather predictions. In Proceedings of the Workshop on the Planetary Boundary Layer, Boulder, CO, USA, 14–18 August 1978.
4. Arya, S.P.S. Suggested revisions to ceratain Boundary Leyer parameterization schemes used in Mosppheric Ciculation Models. *Mon. Weath. Rev.* **1977**, *105*, 215–227.
5. Venkatram, A.; Wyngaard, J.C. *Lectures on Air Pollution Modelling*; American Meteorological Society: Boston, MA, USA, 1988.
6. Pasquill, F. *Atmospheric Diffusion*; Wiley: New York, NY, USA, 1974.
7. Hagemann, S. *An Improved Land Surface Parameter Dataset for Global and Regional Climate Models*; Report No. 336; Max Plank Institute for Meteorology: Hamburg, Germany, 2002.
8. Wieringa, J. Representative roughness parameters for homogeneous terrain. *Bound. Layer Meteorol.* **1993**, *63*, 323–363.
9. Norman, J.M.; Becker, F. Terminology in thermal infrared remote sensing of natural surfaces. *Agric. For. Meteorol.* **1995**, *77*, 153–166.
10. De Bruin, H.A.R.; Verhoef, A. A new method to determine the zero plane displacement. *Bound. Layer Meteorol.* **1997**, *116*, 385–392.
11. Loureiro, J.R.B.; Freire, A.P.S.; Alho, A.T.P.; Ilha, A. The error in origin from first principles. In Proceedings of the International Congress of Mechanical Engineering COBEM, Brasilia, DF, Brazil, 5–9 November 2007.
12. Martano, P. Estimation of Surface Roughness Length and Displacement Height from Single-Level Sonic Anemometer Data. *J. Appl. Meteorol.* **2000**, *39*, 708–715.
13. Businger, J.A.; Wyngaard, J.C.; Izumi, Y.; Bradley, E.F. Flux-Profile relationships in the Atmospheric Surface Layer. *J. Atmos. Sci.* **1971**, *28*, 181–189.
14. Martano, P. Evapotranspiration estimates over non-homogeneous Mediterranean land cover by a calibrated 'critical resistance' approach. *Atmosphere* **2015**, *6*, 255–272.
15. De Leal Oliveira, M.B.; von Randow, C.; Manzi, A.O.; dos Santos Alvala, R.C.; de Souza, A.; Leitão de Miranda, V.B.R.; Deane de Abreu Sá, L. Fluxos turbulentos de energia sobre o Pantanal Mato-Grossense. *Revista Brasileira de Meteorologia* **2006**, *21*, 159–165. (In Portuguese)
16. Mesquita, F.L.L.; Marques Filho, E.P.; Karam, H.A.; Alvalá, R.C.S. Balanço de radiaçao no Pantanal Mato-Grosense durante a estaçao seca. *Revista Brasileira de Meteorologia* **2013**, *28*, 65–74. (In Portuguese)
17. Marques Filho, E.P.; Sá, L.D.A.; Karam, H.A.; Alvalá, R.C.S.; Souza, A.; Pereira, M.M.R. Atmospheric surface layer characteristics of turbulence above the Pantanal wetland regarding the similarity theory. *Agric. For. Meteorol.* **2008**, *148*, 883–892.
18. Zeri, L.M.M.; Abreu Sá, L.D. Scale dependence of coherent structures contribution to the daytime sensible heat flux over Pantanal wetland. *Atmos. Sci. Lett.* **2011**, *12*, 200–206.
19. Martins, H.S.; Abreu Sá, L.D.; Moraes, O.L.L. Low level jets in the Pantanal wetland nocturnal boundary layer—Case studies. *Am. J. Environ. Eng.* **2013**, *3*, 32–47.

20. Kondo, J.; Saigusa, N.; Sato, T. A parameterization of evaporation from bare soil surfaces. *J. Appl. Meteorol.* **1990**, *29*, 385–389.

21. Rana, G.; Katerji, N.; Mastrorilli, M.; el Moujabber, M. A model for predicting actual evapotranspiration under water stress conditions in a Mediterranean region. *Theor. Appl. Climatol.* **1997**, *56*, 45–55.

22. Brock, F.V.; Richardson, S.J. *Meteorological Measurement Systems*; Oxford University Press: Oxford, UK, 2001.

23. Cava, D.; Contini, D.; Donateo, A.; Martano, P. Analysis of short-term closure of the surface energy balance above short vegetation. *Agric. For. Meteorol.* **2008**, *148*, 82–93.

24. Martano, P. Inverse parameter estimation of the turbulent surface layer from single-level data and surface temperature. *J. Appl. Met. Climatol.* **2008**, *47*, 1027–1037.

25. Mesquita, F.L.L.; Marques Filho, E.P.; Souza, R.L.M.; Karam, H.A. Surface Energy Budget over the Pantanal Wetland during the Dry Season. Available online: http://cascavel.ufsm.br/revistas/ojs-2.2.2/index.php/cienciaenatura/article/viewFile/9526/5674 (accessed on 28 May 2015).

26. Aster, R.C.; Borchers, B.; Thurber, C.H. *Parameter Estimation and Inverse Problems*; Academic Press: London, UK, 2005.

27. Hsieh, C.; Katul, G.; Chi, T. An approximate analytical model for footprint estimation of scalar fluxes in thermally stratified atmospheric flows. *Adv. Water Resour.* **2000**, *23*, 765–772.